An Integrated Traveling Salesman and Coverage Path Planning Problem for Unmanned Aircraft Systems

Junfei Xie, Luis Rodolfo Garcia Carrillo, and Lei Jin

***Abstract*—Unmanned Aircraft Systems (UASs) have gained great popularity in land monitoring, 3-D mapping, search and rescue, among others. Existing studies on UAS path planning in these missions consider only a single region to be examined. However, it is frequently encountered that multiple regions need to be considered while performing a real life mission. How to design the optimal path for the UAS to cover multiple regions is then critical. From a strategical point of view, such a problem can be considered as a variant of the traveling salesman problem (TSP) combined and enhanced with the coverage path planning (CPP) problem. Although TSP and CPP have been studied extensively, its combination, which here is given the name TSP-CPP, hasn't received any attention. In this paper, a preliminary study on how to formulate and solve this problem is conducted. Two novel approaches including a grid-based approach and a dynamic programming based approach are introduced to find the (near) optimal solution. Both numerical analysis and simulation studies are conducted to prove and illustrate the optimality and efficiency of the proposed TSP-CPP approaches.**

***Index Terms*—Autonomous systems; Optimization algorithms**

I. Introduction

IN recent years, Unmanned Aircraft Systems (UASs) have been widely applied for land monitoring [1], 3-dimensional mapping [2], surveillance [3], search and rescue [4], among others. In these examples, UASs are used to collect relevant sensory information, or to find targets within a region. To conduct these missions, path planning for UASs is one of the most critical problems to tackle, which is concerned with generating the optimal path that minimizes the cost required to complete the task.

Diverse research has targeted solutions to the path planning problems for a single UAS. For instance, the authors in [5], [6] investigate the shortest path planning problem, aiming at finding the optimal path to a target while avoiding obstacles. When multiple targets are to be visited, UAS path planning can be formulated as a traveling salesman problem (TSP) [7], or more generally a vehicle routing problem (VRP) [8]. The TSP is the simplest and most famous VRP, which seeks an optimal path to visit all targets exactly once. Evolving from TSP, many variants of VRP have been proposed, such as the VRP with time windows [9], capacitated VRP (CVRP) [10], and clustered CVRP [11], etc. In cases when a UAS is assigned to survey a region, the coverage path planning (CPP) problem [12], [13] is formulated, which aims at finding the optimal path, so that the vehicle covers a region completely. Most CPP methods achieve full coverage by first decomposing the region into a set of sub-regions and then applying the exhaustive search or other coverage algorithms such as depth-first search [14].

Path planning for multiple UASs has also been studied. For instance, papers [15], [16] investigate cooperative path planning for multiple UASs to jointly reach a target with minimal cost. The generalization of the TSP to allow multiple salesmen, known as the MTSP, is studied in [17], [18]. VRP for multiple vehicles has also been investigated, such as the heterogeneous fleet VRP [19] and the polygon visiting MTSP (PVMTSP) [20]. In most of these TSP/VRP studies, each target is described by a single location. The PVMTSP model considers polygon regions, but only requires the vehicle to reach the boundary of each region in order to consider such a region a visited one. CPP for a team of UASs has also been studied in [21], [22].

Although UAS path planning has been studied extensively, existing approaches either focus on visiting a set of targets, which can be solved by the shortest path planning [5], [6], TSP or VRP methods [8], or they consider covering a single region, which can be solved by CPP methods [12]. However, scenarios where UASs need to cover multiple regions are quite common. For instance, in post-disaster management, UASs need to assess the damage for multiple disaster-affected areas. In search and rescue missions, targets may be located in multiple spatially distributed regions. A possible solution may consider dispatching one UAS to each region, or randomly selecting the path to cover each region. Unfortunately, under this naive solution, the system can be highly inefficient and cost-expensive. In order to reduce the cost and to enable a broader use of UASs, systematic investigations on this new research topic are crucial.

This paper considers the path planning problem for a single multirotor UAS with sufficient power to cover multiple spatially distributed rectangular regions, as a preliminary study of the proposed new research topic. This problem can be considered as a variant of TSP combined and enhanced with CPP, which aims to determine the optimal path to fully cover all regions exactly once. The combination of TSP and CPP, both of which are NP-hard, introduces significant challenges.

This work was supported by the Texas Comprehensive Research Fund Program Grant.

Junfei Xie (junfei.xie@tamucc.edu), Luis Rodolfo Garcia Carrillo (luis.garcia@tamucc.edu), and Lei Jin (lei.jin@tamucc.edu) are with the Department of Computing Sciences, Department of Engineering, and Department of Mathematics & Statistics, respectively. They are all from Texas A&M University-Corpus Christi, Corpus Christi, TX 78412.

This article has been accepted for publication in a future issue of this journal, but has not been fully edited. Content may change prior to final publication. Citation information: DOI 10.1109/LCSYS.2018.2851661, IEEE Control Systems Letters

In particular, the optimization of inter-regional paths among regions and the optimization of intra-regional paths within each region are nested and cannot be considered separately, making the integrated TSP and CPP (TSP-CPP) problem much more complicated than TSP and CPP. In addition, with points extended to regions, it is also needed to determine the optimal locations for the UAS to enter and exit each region, which impacts the selection of both intra- and inter-regional paths and thus further increases the complexity.

To address the new TSP-CPP problem formulated in Section II, two novel approaches are developed. A simple grid-based approach is first introduced in Section III-A, which finds a (near) optimal solution by converting the TSP-CPP to a basic TSP. To break the curse of dimensionality with respect to the size of the regions, a dynamic programming (DP) based approach is further developed in Section III-B, which explores the selection of entrance and exit locations in each region, and the optimization of intra- and inter-regional paths. Both approaches are proved to be able to find optimal solutions under minor assumptions. Complexity analysis (Section III-C), illustrative examples (Section IV-A) and comparative simulation studies with a Hopfield neural network (NN)-based approach (Section IV-B) demonstrate the efficiency and optimality of the proposed approaches.

II. Problem Formulation

Consider the scenario where a single multirotor UAS that can turn with an arbitrary radius of curvature is assigned to survey N number of non-overlapping spatially distributed rectangular regions. The UAS is assumed to have sufficient power to complete the mission, and to fly at a constant altitude with a constant speed. Therefore, the problem can be formulated in a 2-dimensional space.

For convenience, the regions are labeled with numbers $1, \ldots, N$, and the depot with number 0. Therefore, $\mathcal{N}_0 = \mathcal{N} - \{0\} = \{1, 2, \ldots, N\}$ represents the set of target regions where $\mathcal{N} = \{0, 1, 2, \ldots, N\}$. Region i is characterized by four vertices $\{v_{i1}, v_{i2}, v_{i3}, v_{i4}\}$ and the depot is described by its location v_0. The sensor carried by the UAS is assumed to have a field-of-view or a range of $r \times r$, where r is a positive constant. To describe the path, let $S_i = (s_{im})_{m=1}^{n_i}$ represent an ordered sequence of n_i locations in region $i \in \mathcal{N}_0$, such that the UAS covers region i completely if and only if it moves through all locations in S_i in order. To capture the order of the regions to be visited, a decision variable x_{ij} is introduced, where $x_{ij} = 1$ if the UAS moves from region (or depot) i to region (or depot) j, and $x_{ij} = 0$ otherwise.

The TSP-CPP problem can then be formulated as finding the location sets S_i, $\forall i \in \mathcal{N}_0$ and values of x_{ij}, $\forall i, j \in \mathcal{N}$, such that the path starts and ends at the depot, each region is completely covered exactly once by the UAS, and the total cost z given below is minimized.

$$
\begin{aligned}
z = &\sum_{i \in \mathcal{N}_0} \sum_{j \in \mathcal{N}_0} x_{ij} d(s_{in_i}, s_{j1}) + \sum_{i \in \mathcal{N}_0} \sum_{m=1}^{n_i - 1} d(s_{im}, s_{i(m+1)}) \\
&+ \sum_{i \in \mathcal{N}_0} x_{0i} d(v_0, s_{i1}) + \sum_{i \in \mathcal{N}_0} x_{i0} d(s_{in_i}, v_0) \qquad (1)
\end{aligned}
$$

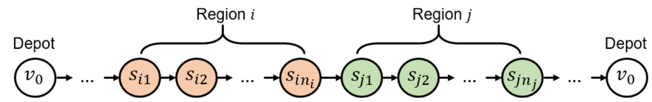

Fig. 1. A candidate path sequence.

where $d(a, b)$ is the travel cost from location a to location b, which is represented here as the Euclidean distance. The first two terms in equation (1) calculate the total travel costs for inter-regional and intra-regional movements. The last two terms calculate the costs for traveling from the depot to the first region in the path and from the last region back to the depot. To ensure the validity of the selected path, the following two constraints are enforced

$$
\begin{aligned}
\sum_{j \in \mathcal{N},\ i \neq j} x_{ij} &= 1, \qquad \forall i \in \mathcal{N}_0 \qquad (2) \\
\sum_{j \in \mathcal{N},\ i \neq j} x_{ij} - \sum_{j \in \mathcal{N},\ i \neq j} x_{ji} &= 0, \qquad \forall i \in \mathcal{N} \qquad (3)
\end{aligned}
$$

The constraint in equation (2) ensures that each region is only visited once, except for the depot. The constraint in equation (3) maintains the continuity of the path. A candidate path sequence is shown in Figure 1 for illustration.

Note that when the size of each region is smaller than or equal to the UAS' sensor range, the TSP-CPP problem is reduced to a TSP, where each region can be simply described by its central location. When there is only one region and the size of the region is larger than the UAS' sensor range, the TSP-CPP problem is reduced to a CPP problem.

III. Solutions to the Integrated TSP-CPP

This section provides solutions to the TSP-CPP problem formulated in Section II. Two approaches are developed: 1) a grid-based approach, and 2) a DP-based approach.

A. Grid-based Approach

The proposed grid-based approach decomposes each region into a collection of grid cells, and then transforms the TSP-CPP problem into a TSP. In particular, each region i is decomposed into a set of uniform grid cells of size $\frac{w_i}{\lceil w_i/r \rceil} \times \frac{h_i}{\lceil h_i/r \rceil}$, where $w_i = \|v_{i2} - v_{i1}\|$ and $h_i = \|v_{i4} - v_{i1}\|$ are the width and height of region i, respectively, and $\|\cdot\|$ represents the L_2-norm operator. The total number of cells in region i is $M_i = \lceil \frac{w_i}{r} \rceil \lceil \frac{h_i}{r} \rceil$. As $\frac{w_i}{\lceil w_i/r \rceil} \leq r$ and $\frac{h_i}{\lceil h_i/r \rceil} \leq r$, the size of each cell is smaller than or equal to the sensor range of the UAS. With each cell regarded as a region, the TSP-CPP problem can be formulated as visiting $M = \sum_{i=1}^{N} M_i$ number of regions, where each region can be fully covered by the sensor range of the UAS. This TSP-CPP problem is thus reduced to a TSP. The problem formulation in equations (1)-(3) still apply if considering each cell as a region. Traditional approaches, such as DP [23], can then be applied to find the optimal path. Theorem 1 shows the optimality of the grid-based approach.

Theorem 1. ***(Optimality of the Grid-based Approach)****. Consider the TSP-CPP problem formulated in equations* (1)-(3).

This article has been accepted for publication in a future issue of this journal, but has not been fully edited. Content may change prior to final publication. Citation information: DOI 10.1109/LCSYS.2018.2851661, IEEE Control Systems Letters

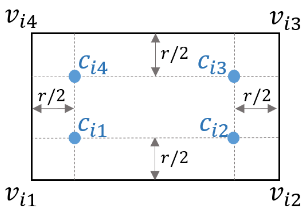

Fig. 2. Example of the four corner points $\{c_{i1}, c_{i2}, c_{i3}, c_{i4}\}$ in region i.

The path found by the grid-based approach is optimal if $\frac{w_i}{\lceil w_i/r \rceil} = \frac{h_i}{\lceil h_i/r \rceil} = r$, $\forall\, i \in \mathcal{N}_0$ *and each grid cell is regarded as a region.*

Proof. If $\frac{w_i}{\lceil w_i/r \rceil} = \frac{h_i}{\lceil h_i/r \rceil} = r$, the size of each cell equals the sensor range of the UAS, which means that the shortest paths to move through the centers of all cells in a region are also the shortest paths to fully cover this region. Therefore, when applying the TSP method that finds the minimum-total-length path passing over all targets, the grid-based approach generates the optimal solution. □

B. DP-based Approach

DP has been widely used to solve the TSP [23]. However, the same procedures cannot be directly applied to tackle the TSP-CPP problem, which requires the optimization for both inter- and intra-regional paths and the selection of entrance and exit locations in each region. This section first discusses the search for optimal intra-regional paths, and then provides the algorithm to solve the TSP-CPP problem using DP.

Note that the starting and ending points of intra-regional paths determine the lengths of inter-regional paths. Therefore, to find the optimal intra-regional path for a region, we need to take its preceding and succeeding regions into the consideration. In this study, the optimization of intra-regional paths is simplified by making the UAS to follow zigzag paths, and by limiting the starting and ending points of intra-regional paths to the corner points c_{iq} defined as

$$c_{iq} = \begin{cases} v_{i1} + \frac{r}{2}\left(n_{hi} + n_{vi}\right) & \text{if} \quad q = 1 \\ v_{i2} - \frac{r}{2}\left(n_{hi} - n_{vi}\right) & \text{if} \quad q = 2 \\ v_{i3} - \frac{r}{2}\left(n_{hi} + n_{vi}\right) & \text{if} \quad q = 3 \\ v_{i4} + \frac{r}{2}\left(n_{hi} - n_{vi}\right) & \text{if} \quad q = 4 \end{cases} \tag{4}$$

where $i \in \mathcal{N}_0$, $q \in A = \{1, 2, 3, 4\}$, $n_{hi} = \frac{v_{i2} - v_{i1}}{w_i}$ and $n_{vi} = \frac{v_{i4} - v_{i1}}{h_i}$. An illustration of the corner points is shown in Figure 2. Two example zigzag paths starting from corner point c_{i4} are shown in Figure 3. Lemma 1 shows that such zigzag paths can fully cover a region with the shortest length.

Lemma 1. *(**Shortest Coverage Distance**). Consider a UAS with a sensor range of* $r \times r$*. To fully cover a rectangular region of size* $w \times h$*, the shortest distance the UAS needs to travel is* $\min\{\lceil \frac{w}{r} \rceil (h - r) + (w - r),\ \lceil \frac{h}{r} \rceil (w - r) + (h - r)\}$.

Proof. When $\frac{w}{\lceil w/r \rceil} = r$ (or when $\frac{h}{\lceil h/r \rceil} = r$), it is easy to prove that the shortest coverage distance is $\frac{wh}{r} - r$. This result can be accomplished by decomposing the region into $\frac{w}{r}$ (or into $\frac{h}{r}$) number of sub-regions of size $r \times h$ (or size $r \times w$), and by making the UAS to follow a zigzag path like the one shown in Figure 3(a) (or Figure 3(b)), which leads to the smallest overlap of covered area. Note that both zigzag paths shown in Figure 3 have the shortest length as both $\frac{w}{\lceil w/r \rceil} = r$ and $\frac{h}{\lceil h/r \rceil} = r$ hold.

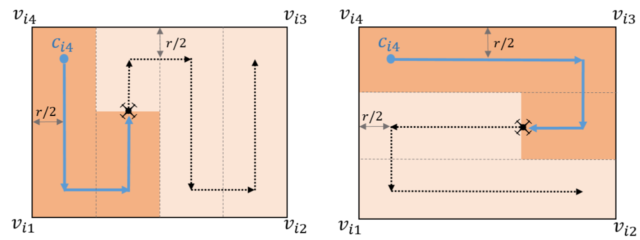

(a) (b)

Fig. 3. Two zigzag paths starting from corner point c_{i4}. Shaded area marked by dark yellow indicates the area already covered. The area that will be covered when the UAS completes the path is marked by light yellow.

In cases when $\frac{w}{\lceil w/r \rceil} \neq r$ and $\frac{h}{\lceil h/r \rceil} \neq r$, the region is decomposed vertically (or horizontally) into two sub-regions of sizes $r(\lceil \frac{w}{r} \rceil - 1) \times h$ and $r(\frac{w}{r} - \lceil \frac{w}{r} \rceil + 1) \times h$ (or of sizes $r(\lceil \frac{h}{r} \rceil - 1) \times w$ and $r(\frac{h}{r} - \lceil \frac{h}{r} \rceil + 1) \times w$) respectively, as shown in Figure 4(a) (or Figure 4(b)). Therefore, the above analysis can be applied to find the shortest coverage distance for the large sub-region, which is $(\lceil \frac{w}{r} \rceil - 1)h - r$ (or $(\lceil \frac{h}{r} \rceil - 1)w - r$). The shortest coverage distance for the small sub-region can also be easily obtained, which is $h - r$ (or $w - r$). The shortest travel distance to move from the large sub-region to the small one is then calculated, which is $w - r(\lceil \frac{w}{r} \rceil - 1)$ (or $h - r(\lceil \frac{h}{r} \rceil - 1)$), as illustrated by the red path in Figure 4(a) (or Figure 4(b)). Summing up the three distance values leads to the length of the complete zigzag path, which is $\lceil \frac{w}{r} \rceil (h - r) + (w - r)$ (or $\lceil \frac{h}{r} \rceil (w - r) + (h - r)$). Therefore, the shortest coverage distance for the whole region is $\min\{\lceil \frac{w}{r} \rceil (h - r) + (w - r),\ \lceil \frac{h}{r} \rceil (w - r) + (h - r)\}$. □

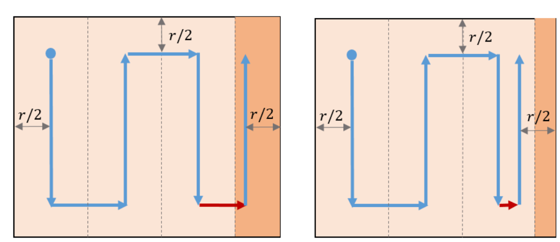

(a) (b)

Fig. 4. Candidates of the shortest zigzag paths to cover regions with $\frac{w}{\lceil w/r \rceil} \neq r$ and $\frac{h}{\lceil h/r \rceil} \neq r$, where each region is decomposed vertically into two sub-regions marked by different colors.

The previous analyses allow finding the shortest zigzag path, given the starting point. Here, let $f(c_{iq}) = S_i$ be the function that finds the shortest zigzag path to cover region i, given c_{iq}, $q \in A$, as the starting point, where S_i includes all turning points along the path, and $s_{i1} = c_{iq}$. Note that s_{in_i} is also a corner point as shown in Figure 4.

This article has been accepted for publication in a future issue of this journal, but has not been fully edited. Content may change prior to final publication. Citation information: DOI 10.1109/LCSYS.2018.2851661, IEEE Control Systems Letters

The use of DP to solve the TSP-CPP problem is now introduced. Let $T \subseteq \mathcal{N}_0$ be a subset of target regions, and define $D(T, i, c_{iq})$, $i \in T$ and $q \in A$, as the length of the shortest path that fully covers each region in T exactly once, starting at the depot and ending at corner point c_{iq} in region i. The calculation of $D(T, i, c_{iq})$ can be broken down into smaller sub-problems. In particular, suppose $k \in T$ is the region visited prior to region i, and let c_{kl}, $l \in A$, be the location where the UAS exits region k. Now, $D(T, i, c_{iq})$ equals the sum of $D(T - \{i\}, k, c_{kl})$ and the length of the shortest path from c_{kl} to c_{iq}, which can be found by applying function $f(c_{iq})$. As k could be any region in $T - \{i\}$ and c_{kl} could be any of the four corner points in region k, $D(T, i, c_{iq})$ is solved by considering all $k \in T - \{i\}$ and all $l \in A$ for each k. The mathematical formulation of $D(T, i, c_{iq})$ is given by

$$D(T, i, c_{iq}) = \begin{cases} g(v_0, c_{iq}) & \text{if } T = \{i\} \\ \infty & \text{if } i \notin T \\ \min\limits_{\substack{k \in T - \{i\} \\ l \in A}} D(T - \{i\}, k, c_{kl}) + g(c_{kl}, c_{iq}) & \text{otherwise} \end{cases} \tag{5}$$

where $g(a, c_{iq})$ calculates the length of the shortest path from location a to c_{iq}, which can be derived from the function $f(c_{iq})$. In particular, $g(a, c_{iq}) = d(a, s_{in_i}) + \sum_{m=1}^{n_i - 1} d(s_{im}, s_{i(m+1)})$ and $S_i = \{s_{i1}, s_{i2}, \ldots, s_{in_i}\} = f(c_{iq})$. The pseudo-code of the proposed DP-based approach is provided in Algorithm 1, where table P keeps track of the locations to be visited along the path. Theorem 2 shows the optimality of the DP-based approach.

Theorem 2. ***(Optimality of the DP-based Approach)****. Consider the TSP-CPP problem formulated in equations* (1)-(3)*. The path found by the DP-based approach in Algorithm 1 is optimal if the UAS can only enter or exit a region from the corner points, and follows zigzag paths like the ones shown in Figure 3 within each region.*

Proof. Theorem 2 can be proved by induction [23] using equation (5). As $D(T, i, c_{iq})$ calculated in each recursion step is the length of the shortest path that ends at c_{iq} in region i and fully covers each region in T exactly once, Line 18 in Algorithm 1 finds the shortest path to cover all regions. □

Algorithm 1: DP-based Approach for TSP-CPP

Input: Depot v_0, vertices of the regions in $\mathcal{N}_0$, and sensor range $r \times r$ of the UAS.
Output: A shortest path that covers all regions in $\mathcal{N}_0$ starting and ending at depot v_0, and its length.

1 **foreach** $i \in \mathcal{N}_0$ **do**
2   **foreach** $q \in A$ **do**
3     $S_i \leftarrow f(c_{iq})$;
4     $D(\{i\}, i, c_{iq}) \leftarrow d(v_0, s_{in_i}) + \sum_{m=1}^{n_i-1} d(s_{im}, s_{i(m+1)})$;
5     $P(\{i\}, i, c_{iq}) \leftarrow (S_i, v_0)$;
6 **foreach** $t = 2, \ldots, N$ **do**
7   **foreach** $T \subseteq \mathcal{N}_0$ *where* $|T| = t$ **do**
8   **foreach** $i \in T$ **do**
9   **foreach** $q \in A$ **do**
10   **foreach** $k \in T - \{i\}$ **do**
11   **foreach** $l \in A$ **do**
12             $S_i \leftarrow f(c_{iq})$;
13             $g(c_{kl}, c_{iq}) \leftarrow d(c_{kl}, s_{in_i}) + \sum_{m=1}^{n_i-1} d(s_{im}, s_{i(m+1)})$;
14             $dist \leftarrow D(T - \{i\}, k, c_{kl}) + g(c_{kl}, c_{iq})$;
15   **if** $dist < D(T, i, c_{iq})$ **then**
16               $D(T, i, c_{iq}) \leftarrow dist$;
17               $P(T, i, c_{iq}) \leftarrow (S_i, c_{kl})$;
18 **return** $\min\limits_{i \in \mathcal{N}_0, q \in A} D(\mathcal{N}_0, i, c_{iq}) + d(v_0, c_{iq})$ *and the shortest path by backtracking over arcs in table* P.

C. Complexity Analysis

This section analyzes the complexity of the proposed approaches, directly addressing their computational efficiency.

1) Complexity of the Grid-based Approach: It is known that the complexity of the basic TSP problem solved by DP is $O(n^2 \cdot 2^n)$, where n is the total number of targets to be visited [23]. As the grid-based approach converts the TSP-CPP problem into a basic TSP with $n = M = \sum_{i=1}^{N} M_i = \sum_{i=1}^{N} \lceil \frac{w_i}{r} \rceil \lceil \frac{h_i}{r} \rceil$, its complexity is $O(M^2 2^M)$, where M grows with the increase of the region size or the number of regions.

2) Complexity of the DP-based Approach: Consider the calculation of $D(T, i, c_{iq})$ in Algorithm 1. For each $T \subseteq \mathcal{N}_0$, $i \in T$, and $q \in A$, $D(T, i, c_{iq})$ can be calculated by considering $|A||T| \leq 4N$ number of sub-problems, where $f(c_{iq})$ in each sub-problem is computed by comparing two possible zigzag paths. As there are a total number of $4 \sum_{i=1}^{N} i \binom{N}{i} = N \cdot 2^{N+1}$ possible combinations of (T, i, c_{iq}), the complexity of the DP-based approach for the TSP-CPP problem is $O(N \cdot 2^{N+1} \cdot 8N) = O(N^2 \cdot 2^N)$, indicating that the DP-based approach is scalable to the region size, but suffers from the curse of dimensionality with respect to the number of regions.

IV. Simulation Studies

This section presents a series of simulation studies to illustrate the optimality and efficiency of the proposed TSP-CPP approaches, which are implemented using Matlab.

A. Optimality Study

Theorems 1 and 2 have proved that both grid-based and DP-based approaches can find optimal solutions under minor assumptions. In this study, two experiments were designed to illustrate the capability of these approaches in finding optimal solutions when their underlying assumptions are satisfied, and also when these assumptions are violated. The grid-based approach uses DP to find the optimal path after cellular decomposition.

The first experiment considers three square regions distributed around the depot with $w_i = h_i = 4$, $\forall i \in \mathcal{N}_0$, where

This article has been accepted for publication in a future issue of this journal, but has not been fully edited. Content may change prior to final publication. Citation information: DOI 10.1109/LCSYS.2018.2851661, IEEE Control Systems Letters

$\mathcal{N}_0 = \{1, 2, 3\}$. The sensor range of the UAS is set to $r = 2$. Therefore, $\frac{w_i}{\lceil w_i/r \rceil} = \frac{h_i}{\lceil h_i/r \rceil} = r$ holds, and the grid-based approach finds the optimal path shown in Figure 5(a), which has the shortest length of 54.3908. As the corner points of each region coincide with the centers of the grid cells defined in the grid-based approach, the DP-based approach also finds the same optimal path shown in Figure 5(a). To illustrate the performance of the grid-based approach when its underlying assumption is violated, the sensor range is increased to $r = 3$, and thus $\frac{w_i}{\lceil w_i/r \rceil} = \frac{h_i}{\lceil h_i/r \rceil} \neq r$. Under this setting, the DP-based approach finds the optimal path of length 49.0141 shown in Figure 5(b), while the grid-based approach generates a sub-optimal path, which is the same as the one shown in Figure 5(a).

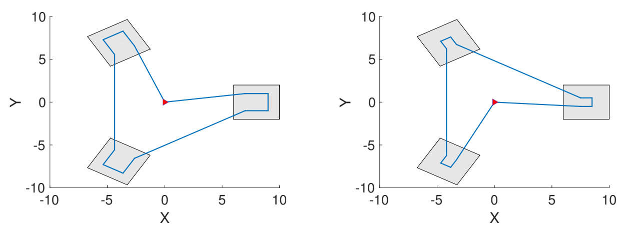

(a) (b)

Fig. 5. Optimal path (blue lines) found by the DP-based approach when a) $r = 2$ and when b) $r = 3$. In both cases, the grid-based approach generates the same path shown in a). Shaded grey areas and the red triangle represent regions and the depot respectively.

As corner points may not be the optimal locations to enter or exit the regions, the DP-based approach may find sub-optimal solutions. To illustrate this situation, the second experiment was designed taking into account three regions as shown in Figure 6, where the size of the largest region is 6×4 and the size of the other two regions is 2×2. The sensor range is set to $r = 2$. As $\frac{w_i}{\lceil w_i/r \rceil} = \frac{h_i}{\lceil h_i/r \rceil} = r$ holds for all $i \in \mathcal{N}_0$ where $\mathcal{N}_0 = \{1, 2, 3\}$, the grid-based approach finds the optimal path of length 34.7660 as shown in Figure 6(a). The DP-based approach finds a sub-optimal path of length 35.0461 as shown in Figure 6(b), which is very close to the optimal solution.

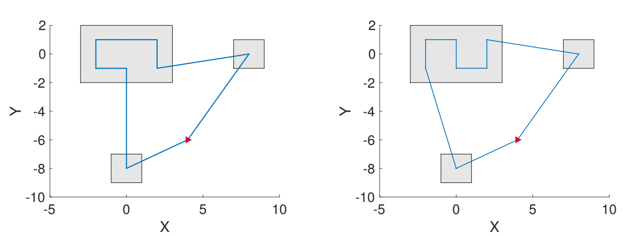

(a) (b)

Fig. 6. Optimal path found by a) the grid-based approach, and b) the suboptimal path found by the DP-based approach.

B. Efficiency Study

Two experiments were designed to investigate the efficiency of the proposed TSP-CPP approaches. For comparison, the Hopfield NN [24], which has been frequently used to solve

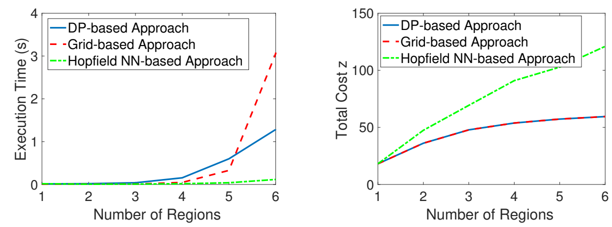

(a) (b)

Fig. 7. Comparison of the a) execution time and b) total cost z generated by the grid-based, the DP-based and Hopfield NN-based approaches with the increase of the number of regions.

TSP with low computational cost, was also implemented and combined with cellular decomposition to find sub-optimal TSP-CPP solutions efficiently. The parameters in the Hopfield NN were configured using the approach introduced in [24]. Each experiment was repeated for 10 times to reduce uncertainty, and the averaged results are presented.

In the first experiment, the efficiency was evaluated under a varying number of regions. Specifically, a collection of uniform regions of size 2×4 is considered, and the sensor range is set to $r = 2$. As shown in Figure 7(a), the execution time of both the DP-based and grid-based approaches grows exponentially with the increase of the number of regions, indicating that both approaches suffer from the curse of dimensionality with regards to the number of regions. The Hopfield NN-based approach is the most efficient, but its accuracy decreases fast with the increase of the number of regions (see Figure 7(b)) as it can easily get stuck at local minima [24].

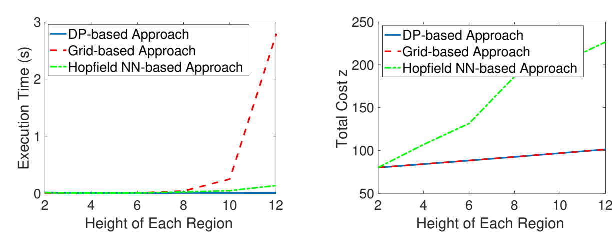

(a) (b)

Fig. 8. Comparison of the a) execution time and b) total cost z generated by the grid-based, the DP-based and Hopfield NN-based approaches with the increase of the height of the regions.

In the second experiment, the efficiency of the three approaches is compared under varying region sizes. In particular, two regions are considered, and the width of each region is fixed to $w_i = 2$, $i \in \{1, 2\}$. The height of each region is then increased simultaneously. As shown in Figure 8(a), the execution time of the DP-based approach remains stable with the increase of the region size, indicating the good scalability to the size of the regions. The grid-based approach suffers from the curse of dimensionality with regards to the region size. The Hopfield NN-based approach is less efficient than the DP-based approach and has low accuracy especially when the region size is large.

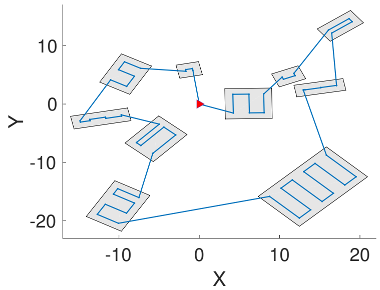

Fig. 9. Optimal path found by the DP-based approach for 10 randomly sized and distributed regions.

C. Large-scale Example

A last experiment was designed to show the capability of the DP-based approach in solving problems of relatively large scale. In this experiment, 10 regions having a width and a height uniformly distributed over the range of $[2,8]$ and $[2,6]$, respectively, are created and randomly distributed in a 2-dimensional area. The sensor range is set to $r = 2$. The optimal path found by the DP-based approach is shown in Figure 9, which is obtained in around 5.7 minutes. The grid-based approach decomposes these regions into total number of $M = 96$ cells, and thus requires $O(96^2 \cdot 2^{98})$ time to find the optimal solution, which is time-prohibitive. Of note, it is suggested to use DP for a TSP of up to 17 targets [23].

V. Conclusions and Future Work

In this paper, a new UAS path planning problem, called the TSP-CPP, is mathematically formulated. Two approaches are then developed to solve this problem, both of which are proved to be able to find the optimal path under minor assumptions. The complexity analysis demonstrates the scalablity of the DP-based approach with respect to the size of the regions. Simulation results illustrate the optimality and efficiency of the proposed TSP-CPP approaches in different scenarios. Future work will investigate more complicated scenarios, such as the existence of obstacles, arbitrarily shaped regions and path planning for fixed-wings with minimum turn radius constraint. Intelligent optimization algorithms, such as reinforcement learning [25], [26] and recurrent neural network [27], [28], to improve the efficiency of the proposed TSP-CPP approaches, and the extension of these results to multi-UAS path planning problems will also be considered.

References

[1] D.-I. Kim, Y.-S. Song, G. Kim, and C.-W. Kim, "A study on the application of uav for korean land monitoring," *Journal of the Korean Society of Surveying, Geodesy, Photogrammetry and Cartography*, vol. 32, no. 1, pp. 29–38, 2014.

[2] F. Nex and F. Remondino, "Uav for 3d mapping applications: a review," *Applied geomatics*, vol. 6, no. 1, pp. 1–15, 2014.

[3] M. Saska, T. Krajnik, and L. Pfeucil, "Cooperative μuav-ugv autonomous indoor surveillance," in *Proceedings of the 9th International Multi-Conference on Systems, Signals and Devices (SSD)*. Chemnitz, Germany: IEEE, March 2012.

[4] F. Muñoz, E. Quesada, E. Steed, H. M. La, S. Salazar, S. Commuri, and L. R. Garcia Carrillo, "Adaptive consensus algorithms for real-time operation of multi-agent systems affected by switching network events," *International Journal of Robust and Nonlinear Control*, vol. 27, no. 9, pp. 1566–1588, 2017.

[5] S. A. Bortoff, "Path planning for uavs," in *Proceedings of American Control Conference*. Chicago, IL: IEEE, June 2000.

[6] X. Gao, Z. Hou, X. Zhu, J. Zhang, and X. Chen, "The shortest path planning for manoeuvres of uav," *Acta Polytechnica Hungarica*, vol. 10, no. 1, pp. 221–39, 2013.

[7] M. Bellmore and G. L. Nemhauser, "The traveling salesman problem: a survey," *Operations Research*, vol. 16, no. 3, pp. 538–558, 1968.

[8] P. Toth and D. Vigo, *The vehicle routing problem*. SIAM, 2002.

[9] X. Li, P. Tian, and S. C. Leung, "Vehicle routing problems with time windows and stochastic travel and service times: Models and algorithm," *International Journal of Production Economics*, vol. 125, no. 1, pp. 137–145, 2010.

[10] D. Mester and O. Bräysy, "Active-guided evolution strategies for large-scale capacitated vehicle routing problems," *Computers & Operations Research*, vol. 34, no. 10, pp. 2964–2975, 2007.

[11] C. Expósito-Izquierdo, A. Rossi, and M. Sevaux, "A two-level solution approach to solve the clustered capacitated vehicle routing problem," *Computers & Industrial Engineering*, vol. 91, pp. 274–289, 2016.

[12] E. Galceran and M. Carreras, "A survey on coverage path planning for robotics," *Robotics and Autonomous systems*, vol. 61, no. 12, pp. 1258–1276, 2013.

[13] A. Khan, E. Yanmaz, and B. Rinner, "Information exchange and decision making in micro aerial vehicle networks for cooperative search," *IEEE Transactions on Control of Network Systems*, vol. 2, no. 4, pp. 335–347, 2015.

[14] H. Choset, "Coverage for robotics–a survey of recent results," *Annals of mathematics and artificial intelligence*, vol. 31, no. 1-4, pp. 113–126, 2001.

[15] J. S. Bellingham, M. Tillerson, M. Alighanbari, and J. P. How, "Cooperative path planning for multiple uavs in dynamic and uncertain environments," in *Proceedings of the 41st IEEE Conference on Decision and Control*. Las Vegas, NV: IEEE, December 2002.

[16] P. Chandler, S. Rasmussen, and M. Pachter, "Uav cooperative path planning," in *Proceedings of AIAA Guidance, Navigation, and Control Conference and Exhibit*, Denver, CO, August 2000.

[17] A. I. Ali and J. L. Kennington, "The asymmetric m-travelling salesmen problem: A duality based branch-and-bound algorithm," *Discrete Applied Mathematics*, vol. 13, no. 2-3, pp. 259–276, 1986.

[18] M. Goldstein, "Self-organizing feature maps for the multiple travelling salesmen problem ({MTSP})," in *Proceedings of International Neural Network Conference*, Paris, France, July 1990.

[19] M. Gendreau, G. Laporte, C. Musaraganyi, and É. D. Taillard, "A tabu search heuristic for the heterogeneous fleet vehicle routing problem," *Computers & Operations Research*, vol. 26, no. 12, pp. 1153–1173, 1999.

[20] A. Sathyan, N. D. Ernest, and K. Cohen, "An efficient genetic fuzzy approach to uav swarm routing," *Unmanned Systems*, vol. 4, no. 02, pp. 117–127, 2016.

[21] K. Easton and J. Burdick, "A coverage algorithm for multi-robot boundary inspection," in *Proceedings of the IEEE International Conference on Robotics and Automation*. Barcelona, Spain: IEEE, April 2005.

[22] I. A. Wagner, Y. Altshuler, V. Yanovski, and A. M. Bruckstein, "Cooperative cleaners: A study in ant robotics," *The International Journal of Robotics Research*, vol. 27, no. 1, pp. 127–151, 2008.

[23] R. Bellman, "Dynamic programming treatment of the travelling salesman problem," *Journal of the ACM (JACM)*, vol. 9, no. 1, pp. 61–63, 1962.

[24] K. C. Tan, H. Tang, and S. S. Ge, "On parameter settings of hopfield networks applied to traveling salesman problems," *IEEE Transactions on Circuits and Systems I: Regular Papers*, vol. 52, no. 5, pp. 994–1002, 2005.

[25] M. Jafari, H. Xu, and L. R. G. Carrillo, "Brain emotional learning-based intelligent controller for flocking of multi-agent systems," in *Proceedings of American Control Conference (ACC)*. Seattle, WA: IEEE, May 2017.

[26] J. Xie, Y. Wan, K. Mills, J. J. Filliben, and F. Lewis, "A scalable sampling method to high-dimensional uncertainties for optimal and reinforcement learning-based controls," *IEEE control systems letters*, vol. 1, no. 1, pp. 98–103, 2017.

[27] S. Qin, X. Le, and J. Wang, "A neurodynamic optimization approach to bilevel quadratic programming," *IEEE transactions on neural networks and learning systems*, vol. 28, no. 11, pp. 2580–2591, 2017.

[28] Y. Wang, L. Cheng, Z.-G. Hou, J. Yu, and M. Tan, "Optimal formation of multirobot systems based on a recurrent neural network," *IEEE transactions on neural networks and learning systems*, vol. 27, no. 2, pp. 322–333, 2016.